

Enhanced electron capture and symmetrized carrier distribution in GaInN light-emitting diodes having tailored barrier doping

Di Zhu (朱迪),¹ Ahmed N. Noemaun,¹ Martin F. Schubert,¹ Jaehee Cho,¹ E. Fred Schubert,^{1,a)} Mary H. Crawford,² and Daniel D. Koleske²

¹Department of Physics, Applied Physics, and Astronomy and Department of Electrical, Computer, and Systems Engineering, Future Chips Constellation, Rensselaer Polytechnic Institute, Troy, New York 12180, USA

²Sandia National Laboratories, Albuquerque, New Mexico 87185, USA

(Received 22 January 2010; accepted 3 March 2010; published online 25 March 2010)

The confinement of electrons to the active region of GaInN light-emitting diodes (LEDs) is limited by the (i) inefficient electron capture into polar quantum wells, (ii) electron-attracting properties of electron-blocking layers (EBL), (iii) asymmetry in electron and hole transport, and (iv) unfavorable p-doping in the EBL for high Al content. To counteract these mechanisms, we employ tailored Si-doping in the quantum barriers (QBs). Experiments show a 37.5% enhancement in light-output power at high currents of one-QB-doped LEDs over all-QB-doped LEDs. These results are consistent with simulations showing that QB doping can be used to symmetrize the electron and hole distribution. © 2010 American Institute of Physics. [doi:10.1063/1.3371812]

The “efficiency droop,” which is the gradual decrease of the power efficiency as the injection current increases, was shown to be a unique characteristic of GaN-based multiple-quantum-well (MQW) light-emitting diodes (LEDs). The origin of the high-power loss mechanism remains under active investigation. Several loss mechanisms have been suggested, including electron leakage out of the MQW active region,^{1–3} low hole injection,^{4–6} Auger recombination,^{7,8} carrier delocalization occurring at high excitation intensities,^{9,10} and junction heating.¹¹ For blue LEDs injected with high current densities, the physical mechanism causing the efficiency droop was found to be the single largest loss mechanism.² Therefore the mitigation of the efficiency droop may enable the pervasive market penetration of solid-state-lighting technologies.

The polarization properties of GaInN heterostructures strongly impact carrier transport in ways that likely contribute to efficiency droop. Electron leakage out of the active region can be caused by insufficient electron capture into quantum wells (QWs), especially for polar GaInN QWs with unequal quantum barrier (QB) heights, as illustrated in Fig. 1(a). From a semiclassical view, for an electron to be captured when propagating through a QW, its energy-loss rate (dE/dx) must exceed the potential drop across the QW, that is $dE/dx|_{\text{LO-phonon}} > e\mathcal{E}_{\text{QW}}$ where \mathcal{E}_{QW} is the polarization field in the QW. Assuming that electrons propagate at saturation velocity (1×10^7 cm/s), one can estimate the energy lost by emission of LO phonons ($h\nu_{\text{LO}}=92$ meV) with a phonon emission lifetime of $\tau_{\text{LO}}=10\text{--}200$ fs.^{12,13} For a QW width of $L_{\text{QW}}=3$ nm, one obtains $dE/dx|_{\text{LO-phonon}} < e\mathcal{E}_{\text{QW}}$ indicating that capture of electrons may be difficult. This is particularly relevant for the last (p-side) QW because of the electron-extracting down-sloped band edge of the spacer layer adjoining the right-hand side of the last QW. For non-polarized structures, any energy loss will suffice to capture an electron since $\mathcal{E}_{\text{QW}}=0$. Accordingly, polarization-matched GaInN/

AlGaInN and GaInN/GaN structures have been demonstrated with higher light-output power and less efficiency droop at high currents.^{3,14} In addition, as shown in Fig. 1(b), a positive sheet charge exists at the spacer-to-electron-blocking-layer (EBL) interface due to spontaneous and piezoelectric polarization effects. The corresponding electric field in the spacer layer attracts electrons and drives them out of the active region toward the EBL. Decreasing electron leakage by increasing the Al content in the EBL is counteracted by the simultaneously increasing positive sheet charge at the active-region-EBL interface which further promotes electron extraction.

In addition to these polarization-induced effects, the low hole mobility in GaN (~ 10 cm²/V s) and the more favorable values for electrons (~ 300 cm²/V s), in conjunction with the large thermal activation energy for acceptor ionization (~ 200 meV), result in an inherent asymmetry in electron and hole transport. This asymmetry causes electrons to more easily traverse the MQW active region than holes and reduces hole injection into the active region. As a result, the distribution of electrons and holes within the MQW was found to be highly non-uniform with the p-side end of the MQW active region contributing the majority of radiative recombination events.¹⁵ Thus, while polarization-matched structures have demonstrated reduced efficiency droop and

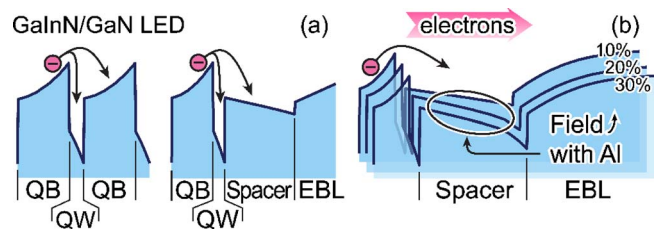


FIG. 1. (Color online) (a) Band diagrams and energy loss of electrons injected into a regular QW and into the very last QW (located next to the EBL); (b) Simulated band diagrams showing increasing field in spacer layer and increasing positive sheet charge at the spacer-to-EBL interface as the EBL Al contents increase from 10% to 20% to 30%.

^{a)}Author to whom correspondence should be addressed. Electronic mail: efschubert@rpi.edu.

other benefits,^{3,14} carrier transport remains strongly asymmetric in such structures; it cannot be fully counteracted by increasing the Al content in the EBL due to the lower p-type doping efficiency at high Al contents.

Based on these reasons, we conclude that the last QW is indeed a “problem QW” that causes electrons to leak away thereby contributing to the efficiency droop. This motivates the pursuit of “inverted” LED structures (n-side-up growth or growth on N-face surfaces),¹⁶ polarization-matched LED structures,^{3,15} wider QW LED structures,⁷ and other LED structures that prevent carriers from recombining mostly in the last QW.¹⁷ Here, we show that this goal can indeed be accomplished by “engineering” the doping profile in the QBs. This strategy is shown to dramatically enhance the light-output power and reduce the efficiency droop.

Si-doped QBs, in general, have been widely used in conventional GaInN LEDs (Ref. 18) and previous studies have indicated that the carrier transport characteristics and the device ideality factor have close relationships with Si doping of the QBs.¹⁹ In the present work, we investigate the carrier transport, distribution, recombination as well as the efficiency droop in GaInN LEDs with different numbers of doped QBs.

The four GaInN/GaN MQW LEDs used in this study are grown on sapphire substrates by metal-organic vapor-phase epitaxy. The GaInN/GaN MQW active region consists of five 2.5-nm-thick Ga_{0.85}In_{0.15}N QWs with four 8.2-nm-thick GaN QBs in between the the QWs. The active region is grown on a 3 μm thick Si-doped n-type GaN layer, and is followed by a 20–30-nm-thick GaN spacer layer, an AlGaIn EBL, and a p-type GaN cladding layer. The four MQW LEDs are distinguished by the number of QBs that are intentionally Si-doped, and we employ doping in 1, 2, 3, and 4 of the QBs, counting from the n-type GaN side. A barrier-doping level of $n \approx 3 \times 10^{18} \text{ cm}^{-3}$ is determined by Hall-effect measurements of thick reference GaN layers grown under the same conditions as the doped QBs. The four LED wafers are processed into lateral LED chips, $300 \times 300 \mu\text{m}^2$ in size, and left unencapsulated. To obtain the L - I - V characteristics of the LEDs, devices are tested from each GaInN/GaN MQW wafer at room temperature and with currents up to 1000 mA. The current sweep is performed in pulsed mode with a 5 μs pulse duration and a 1% duty cycle to prevent self-heating.

Figure 2(a) shows the light-output power of the four LEDs as a function of the forward current I_f . The light-output power of all LEDs increases sublinearly with current. The 4-QB-doped sample shows the lowest light-output power at high currents (>100 mA). As fewer QBs are doped, the light-output power gradually increases. At the maximum forward current of 1000 mA, the 1-QB-doped LED has a 37.5% increase in the light-output power compared to the 4-QB-doped LED. The normalized external quantum efficiency (EQE) versus current is plotted in Fig. 2(b) for the four LED structures. The 4-QB-doped sample has a sharp peak in efficiency, which occurs at a current level below 10 mA; at higher currents, the efficiency rapidly decreases and drops to 40% of its peak value as the current reaches 1000 mA. In contrast, the efficiency peak becomes less sharp as fewer QBs are doped, and the EQE of the 1-QB-doped sample outperforms the 4-QB-doped sample at a current level as low as 50 mA. While the maximum efficiencies for the fewer-QB-doped LEDs (with 1, 2, and 3 doped QBs) are lower than

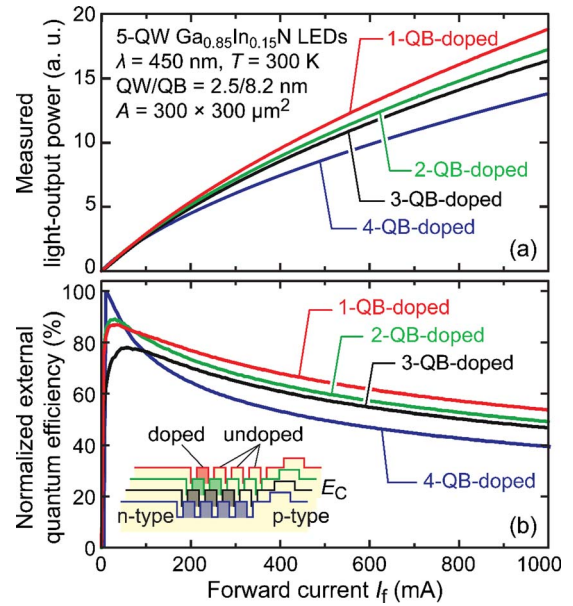


FIG. 2. (Color online) Measured light-output power as a function of forward current of LEDs with different number of doped QBs. (b) Measured EQE as a function of forward current of LEDs with different number of doped QBs normalized to the maximum EQE of the 4-QB-doped structure.

that of the 4-QB-doped LEDs, the maximum efficiencies occur at higher forward currents. The efficiency droop of the fewer-QB-doped LED samples is dramatically reduced.

To understand the mechanism responsible for the increase of high-current EQE and reduced efficiency droop with fewer doped QBs, numerical simulations of the LED structures are performed using APSYS modeling software. The simulation parameters can be found in our previous work,¹⁸ and the conduction-to-valence-band offset ratio is set to be 67:33. The band diagrams corresponding to a forward current of 1000 mA for the 4-QB-doped and 1-QB-doped structures are plotted in Figs. 3(a) and 3(b), respectively. Doping the QBs n-type generally causes a positive curvature of the band edge of the QBs. The lower QB height presents less impedance for well-to-well electron transport. However,

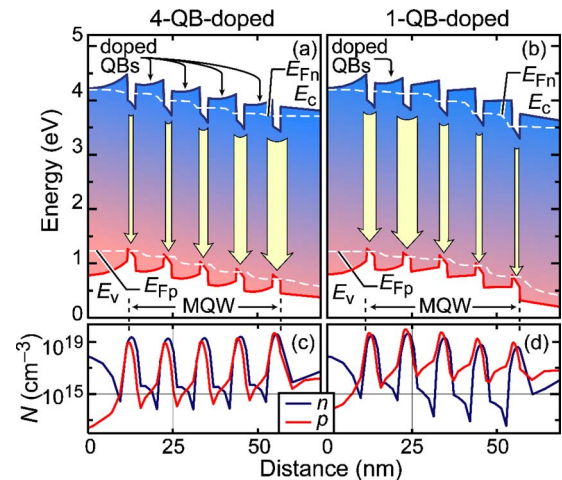


FIG. 3. (Color online) Simulated band profiles and illustration of the distribution of radiative recombination (arrows) within the MQW of GaInN/GaN LEDs with (a) 4-QB-doped ($N_D = 3 \times 10^{18} \text{ cm}^{-3}$) and (b) 1-QB-doped structures at a forward current of 1 A (current density $\sim 1.1 \text{ kA/cm}^2$). Corresponding electron and hole concentration in the MQW active region for the (c) 4-QB-doped and (d) 1-QB-doped structures.

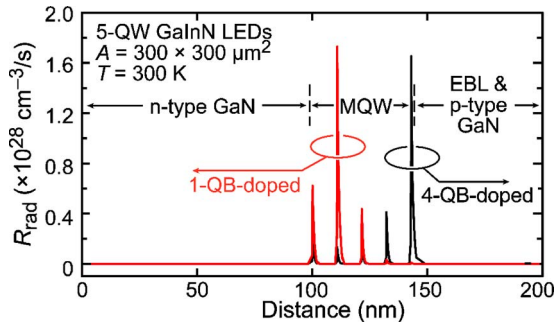


FIG. 4. (Color online) Calculated distribution of radiative recombination in LEDs with 4-QB-doped and 1-QB-doped active-region structures.

holes are impeded from propagating between QWs by the raised QBs in the valence band. Both the electron and hole concentration are highest in the last QW, as shown in Fig. 3(c). This high concentration in the last QW can induce undesired electron leakage and other mechanisms including Auger recombination. Meanwhile, such an electron-favoring transport leads to the strongest radiative recombination in the last QW as depicted in Fig. 3. In contrast, when only the first QB is doped, the asymmetry of electron and hole transport is reduced. The maximum electron and hole concentration is shifted from the last QW to the second QW as shown in Fig. 3(d). Simulation indicates that this hole-favoring transport reduces electron leakage into the p-type GaN, and results in the second QW contributing the most to optical emission as shown in Fig. 4.

To minimize electron leakage, a uniform carrier transport and distribution in the MQWs is preferred. Such a uniform carrier distribution can indeed be attained in simulations by fine tuning the QB doping between electron- and hole-favoring transport as shown in Figs. 5(a) and 5(b). An example of uniform radiative recombination inferred from simulation is shown in Fig. 5(c). By engineering the Si-doping levels in the individual QBs, one can symmetrize carrier transport and more evenly distribute carriers among the QWs, allowing for optimization of GaInN/GaN LEDs.

In summary, we have shown that the inefficient electron capture, the electron-attracting properties of polarized EBL, the inherent asymmetry in electron and hole transport and the

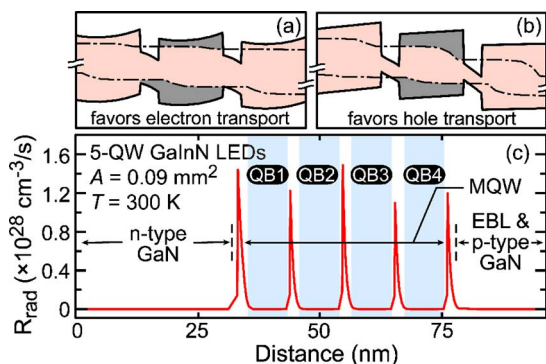


FIG. 5. (Color online) Schematic illustration of the (a) QB-doped structure ($N_D = 6 \times 10^{18} \text{ cm}^{-3}$) that favors electron transport and (b) QB-undoped structure that favors hole transport. The gray shaded regions highlight key differences in the QB band profiles. (c) Calculated radiative recombination showing that a uniform distribution of radiative recombination among the MQWs can be obtained by adjusting the doping in the QBs (QB1: $N_D = 6 \times 10^{18} \text{ cm}^{-3}$; QB2: $N_D = 2 \times 10^{18} \text{ cm}^{-3}$; QB3: $N_D = 2 \times 10^{18} \text{ cm}^{-3}$; QB4: $N_D = 1.4 \times 10^{18} \text{ cm}^{-3}$).

inefficient EBL p-doping at high Al contents severely limit the ability to confine electrons to the MQW active region. We have demonstrated GaInN/GaN MQW blue LEDs employing tailored Si doping in the QBs with strongly enhanced high-current efficiency and reduced efficiency droop. Compared with 4-QB-doped LEDs, 1-QB-doped LEDs show a 37.5% increase in light-output power at high currents. Consistent with the measured results, simulation shows a shift of radiative recombination among the MQWs and a reduced electron leakage current into the p-type GaN when fewer QBs are doped. The results can be attributed to a more symmetric carrier transport and uniform carrier distribution which help to reduce electron leakage and thus reduce the efficiency droop.

The authors gratefully acknowledge support by Sandia's Solid-State Lighting Science Center, an Energy Frontier Research Center funded by the U. S. Department of Energy, Office of Science, Office of Basic Energy Sciences. Sandia is a multiprogram laboratory operated by Sandia Corporation, a Lockheed Martin Co., for the United States Department of Energy's National Nuclear Security Administration under Contract No. DE-AC04-94AL85000. It is also a pleasure to acknowledge technical support by Professor Jong Kyu Kim at Pohang University of Science and Technology.

- ¹M. H. Kim, M. F. Schubert, Q. Dai, J. K. Kim, E. F. Schubert, J. Piprek, and Y. Park, *Appl. Phys. Lett.* **91**, 183507 (2007).
- ²M. F. Schubert, S. Chhajed, J. K. Kim, E. F. Schubert, D. D. Koleske, M. H. Crawford, S. R. Lee, A. J. Fischer, G. Thaler, and M. A. Banas, *Appl. Phys. Lett.* **91**, 231114 (2007).
- ³M. F. Schubert, J. Xu, J. K. Kim, E. F. Schubert, M. H. Kim, S. Yoon, S. M. Lee, C. Sone, T. Sakong, and Y. Park, *Appl. Phys. Lett.* **93**, 041102 (2008).
- ⁴J. Xie, X. Ni, Q. Fan, R. Shimada, U. Ozgur, and H. Morkoc, *Appl. Phys. Lett.* **93**, 121107 (2008).
- ⁵I. V. Rozhansky and D. A. Zakheim, *Phys. Status Solidi A* **204**, 227 (2007).
- ⁶I. A. Pope, P. M. Smowton, P. Blood, J. D. Thomson, M. J. Kappers, and C. J. Humphreys, *Appl. Phys. Lett.* **82**, 2755 (2003).
- ⁷Y. C. Shen, G. O. Müller, S. Watanabe, N. F. Gardner, A. Munkholm, and M. R. Krames, *Appl. Phys. Lett.* **91**, 141101 (2007).
- ⁸N. F. Gardner, G. O. Müller, Y. C. Shen, G. Chen, S. Watanabe, W. Götz, and M. R. Krames, *Appl. Phys. Lett.* **91**, 243506 (2007).
- ⁹A. Y. Kim, W. Götz, D. A. Steigerwald, J. J. Wierer, N. F. Gardner, J. Sun, S. A. Stockman, P. S. Martin, M. R. Krames, R. S. Kern, and F. M. Steranka, *Phys. Status Solidi A* **188**, 15 (2001).
- ¹⁰S. F. Chichibu, T. Azuhata, M. Sugiyama, T. Kitamura, Y. Ishida, H. Okumura, H. Nakanishi, T. Sota, and T. Mukai, *J. Vac. Sci. Technol. B* **19**, 2177 (2001).
- ¹¹A. A. Efremov, N. I. Bochkareva, R. I. Gorbunov, D. A. Larinovich, Yu. T. Rebane, D. V. Tarkhin, and Yu. G. Shreter, *Semiconductors* **40**, 605 (2006).
- ¹²N. M. Stanton, A. J. Kent, A. V. Akimov, P. Hawker, T. S. Cheng, and C. T. Foxon, *J. Appl. Phys.* **89**, 973 (2001).
- ¹³H. Ye, G. W. Wicks, and P. M. Fauchet, *Appl. Phys. Lett.* **74**, 711 (1999).
- ¹⁴J. Xu, M. F. Schubert, A. N. Noemaun, D. Zhu, J. K. Kim, E. F. Schubert, M. H. Kim, H. J. Chung, S. Yoon, C. Sone, and Y. Park, *Appl. Phys. Lett.* **94**, 011113 (2009).
- ¹⁵A. David, M. J. Grundmann, J. F. Kaeding, N. F. Gardner, T. G. Mihopoulos, and M. R. Krames, *Appl. Phys. Lett.* **92**, 053502 (2008).
- ¹⁶M. L. Reed, E. D. Readinger, H. Shen, M. Wraback, A. Syrkina, A. Usikov, O. V. Kovalenkov, and V. A. Dmitriev, *Appl. Phys. Lett.* **93**, 133505 (2008).
- ¹⁷M. Peter, A. Lausch, P. Strauss, A. Walter, J. Bauer, and B. Han, *Phys. Status Solidi C* **5**, 2050 (2008).
- ¹⁸M. Koike and S. Asami, U.S. Patent No. 6,288,416 (1999).
- ¹⁹D. Zhu, J. Xu, A. N. Noemaun, J. K. Kim, E. F. Schubert, M. H. Crawford, and D. D. Koleske, *Appl. Phys. Lett.* **94**, 081113 (2009).